Magazine of Civil Engineering. 2019. 86(2). Pp. 92–104
Инженерно-строительный журнал. 2019. № 2(86). С. 92–104

Magazine of Civil Engineering

ISSN 2071-0305

journal homepage: http://engstroy.spbstu.ru/

DOI: 10.18720/MCE.86.9

Behaviour of axisymmetric thick plates resting against conical surface

V.I. Morozov*, E.K. Opbul, P. Van Phuc,
St. Petersburg State University of Architecture and Civil Engineering, St. Petersburg, Russia
** E-mail: morozov@spbgasu.ru*

Keywords: high-pressure casing; end element; axisymmetric plate; bearings; walls (structural partitions); internal pressure; loads (forces); key; conical surface.

Abstract. The present article is dedicated to analytical and numerical investigation of behavior of end elements of high-pressure casings for nuclear reactors. Nuclear energy generated inside the high-pressure casings will become an actual power-related choice of the human kind in the very near future. In this respect, development of methodology for proper calculation of axisymmetric plates resting against conical surface and bearing the evenly distributed load is becoming state of the art issue. In order to perform analytical calculation the authors used established concrete strength criteria and prerequisites assumed, while ANSYS WORKBENCH software package was applied to calculate the ultimate load value and stress state. Calculations were made considering a keyed connection between thick plate and load-bearing wall of the high-pressure casing and referring to considerably high, in one case, and low (variable), in the other case, plate stiffness. The article presents comparative analysis of calculation results that demonstrates calculation methods adequacy. The authors developed original methods of analytical and numerical calculations allowing to investigate stress state of end elements designed in the form of axisymmetric plates resting against conical surfaces. End elements behavior in load condition is characterized by formation of spheric vault where stress condition typical for concrete three-dimensional compression state occurs. Investigations presented show that sudden disintegration does not occur when concrete end elements are affected by cracks in the stretched area; instead, the spheric vault is formed. Strength of such spheric vault occurring in the element is rather depending upon load bearing wall stiffness, i.e. the lower the stiffness the smaller the strength and vice versa. The following scientific results have been obtained: – end elements shaped as thick axisymmetric plates in condition of ultimate load are characterized by spheric vault formation; -authors, based on assumptions and guided by approximate procedure have obtained the formula for spheric vault thickness calculation; – authors obtained original methods of analytical and numerical calculation to evaluate stress condition of high-pressure casings' end elements shaped as thick axisymmetric plates resting against conical surface; – comparison of calculation results displays minor discepancies between analytical and numerical calculation models.

1. Introduction

Problems associated with experimental-theoretical investigation of buildings and facilities locating hazardous production cycles are still regarded as topical issues which are represented by a wide range of design solutions. Alongside with [1–5], a particular place is held by nuclear reactor high pressure casings – special units in which the process is characterized by high internal pressure, temperature and radiation impacts.

It is a well-known fact [6–10], that NR steel casings have small active zone area dimensions and low parameters of reactor heat carrier, besides, they are very complicated in manufacturing which can be accomplished only in factory conditions. At that, in order to manufacture the casing it is required to prepare a number of ingots made of high-quality electric furnace (pearlitic) steel.

Morozov, V.I., Opbul, E.K., Van Phuc, P. Behaviour of axisymmetric thick plates resting against conical surface. Magazine of Civil Engineering. 2019. 86(2). Pp. 92–104. DOI: 10.18720/MCE.86.9.

Морозов В.И., Опбул Э., Ван Фук Ф. Работа осесимметричных толстых плит, опертых по конической поверхности // Инженерно-строительный журнал. 2019. № 2(86). С. 92–104. DOI: 10.18720/MCE.86.9

In 1959, in France, first nuclear reactors designed in the form pre-stressed concrete structure with active casing in the form of thick-walled (3 meters) horizontal (20 meters diameter) cylinder were built. End elements were made in the form of concave hemispheres to avoid any tension zones caused by internal pressure while lateral pressure, longitudinal and ring tensions were withstood by hooped and longitudinal pre-stressed reinforcements. Steel 3 cm thick leak proof cladding was installed inside the casing.

Despite the fact that pre-stressed reinforced concrete is known to be rather reliable it is necessary to underline that pre-stressing technology is becoming more and more complicated due to technical complexity of structures under design, structures and elements atypicality etc. [11–15].

High-pressure casings of structural solution under design and investigation is a complicated multi-component facility (refer to Figure 1) which includes load-bearing walls made of heavy armored cement [16], plug-type end elements protected from displacement by means of special keys and other structural components which are not covered by this article.

Heavy armored cement is fiber reinforced concrete with large (20 % volume and over)content of small diameter reinforcement rods. First heavy armored cement was invented in 1970s [16, 17].

This article is addressing behavior of axisymmetric thick plates resting against conical surface and bearing the evenly distributed load.

As it is known [17] thick plates may be used in the end parts of high-pressure casings. They are generally known as end elements.

Purpose of this article is to investigate behavior of end elements affected by evenly distributed load with reference to (i) resting state and (ii) stiffness of the casing load bearing wall. Where analytical problem was solved on the basis of classic theory of plastic behavior we made use of “Mathcad 15” software package while numerical computation required ANSYS WorkBench R18.1 software package.

Purpose of this article is (i) to create analytical and numerical methods of assessment of stress-strain behavior (SSB) and (ii) to determine the ultimate load value.

As it is known [16], cracked thick axisymmetric plate being in volumetric strain condition, at loads near to ultimate, is affected by considerably high area of omnidirectional compression, i.e. by a kind of “dome”. If you imagine the thick axisymmetric plate being in plane deformation state it means that the compressed spacial “dome” will take the shape of plane spheric “vault” which will cause “arcuated” behavior of the structure.

2. Methods

Figure 1 presents original structure of cylindrical high-pressure casing made of heavy armored cement [16, 17], in which special key is provided with a purpose to avoid plate displacement against the load-bearing wall.

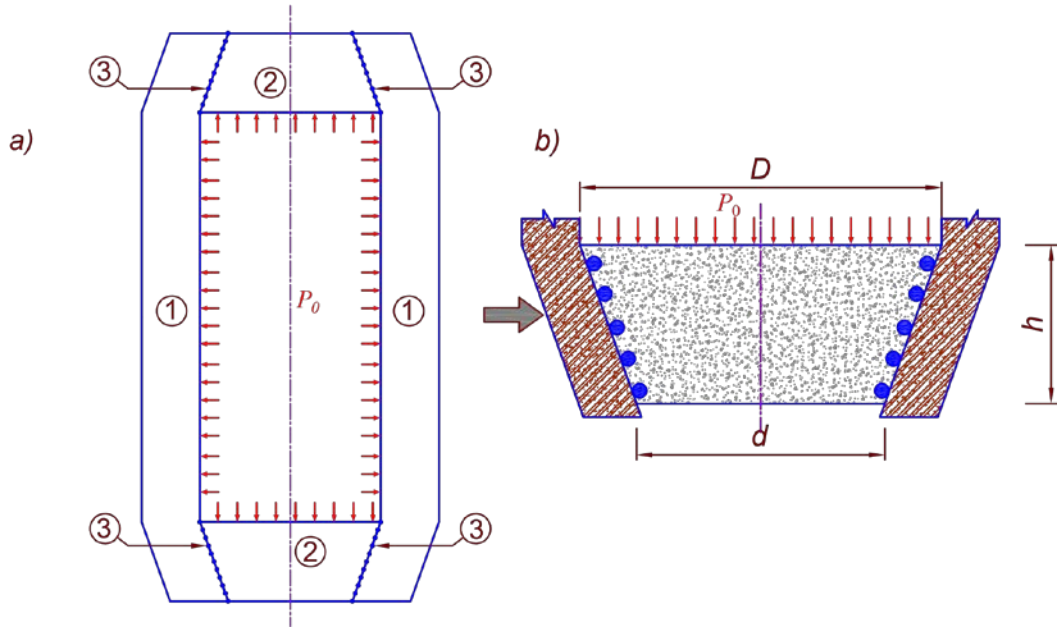

Figure 1. Structural layouts:
a) High-pressure casing: 1 is load bearing wall made of heavy armored cement, 2 is end element, 3 is keys, P_0 is evenly distributed load; b) end elements designed in the form of thick plate: D is largest diameter of the end elements, d is smallest diameter of the end elements, h is height of the end elements.

Below presented are several models of end elements calculation for the case where connection with high-pressure casing made of heavy armored cement is provided by means of the key, inter alia, calculation models depending on wall stiffness.

At the first stage we analyzed axisymmetric concrete thick plate abutting with load bearing wall through the key; at that, it was conditionally assumed that load bearing wall had rather high stiffness. Taking into account the accepted key-type connection between structural elements and casing load-bearing wall – calculation model of the end elements (for plane deformation state) may be viewed from Figure 2.

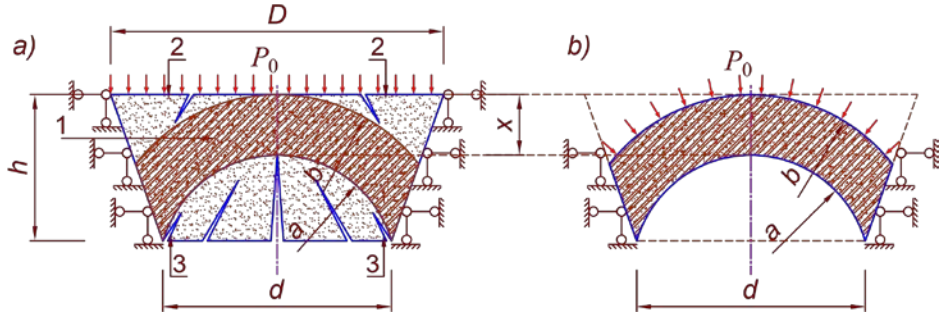

Figure 2. Calculation model for concrete end element with load bearing wall having high stiffness: a) during crack formation stage: 1 is spheric vault, 2 is tension are near supports, 3 is cracks, a is internal diameter of the vault, b is external diameter of the vault, b) during spheric vault crack formation stage.

Obviously, there are practically no radial displacements where load bearing wall is stiff. However, it may be admitted that prior to crack formation the thick wall is operating according to beam pattern.

For thick wall, prior to first cracks formation in plane deformation state, in order to calculate height of compression area it is necessary to assume the following allowances:

- thick concrete element (prior to crack formation) is operating according to beam pattern;
- flat cross-section hypothesis is valid;
- tension area is in the stage of plastic deformations, and ultimate value of plastic deformation is $\varepsilon_{bt2} = 15 \cdot 10^{-5}$;
- compression area is within the elastic behavior zone.

With consideration of accepted assumptions, Figure 3 presents calculation model of thick concrete element prior to first crack formation.

With provision for equilibrium conditions $\Sigma X = 0$ we obtain:

$$R_{bt}(h-x) - \frac{1}{2}\sigma_b x = 0\,. \tag{1}$$

From relations balance $\frac{\varepsilon_b}{\varepsilon_{bt}} = \frac{x}{h-x}$ we obtain

$$\varepsilon_b = \frac{\varepsilon_{bt} x}{h-x}. \tag{2}$$

Using Hooke's law for elastic cross-section zone $\sigma_b = \varepsilon_b E_b$, and taking into account (2) we obtain

$$\sigma_b = \frac{\varepsilon_{bt} x}{h-x} E_b. \tag{3}$$

Jointly solving equations (1) and (3) we obtain formula enabling compression area height (vault thickness) determination:

$$x = \frac{h - \sqrt{h^2 - h^2\left(1 - \frac{\varepsilon_{bt} E_b}{2R_{bt}}\right)}}{1 - \frac{\varepsilon_{bt} E_b}{2R_{bt}}}. \tag{4}$$

Figure 4 presents end elements pattern designed in the form of conic-shape thick plate limited by points *ABCD*, where $GE = x$ – thickness or height of the vault determined by formula (4).

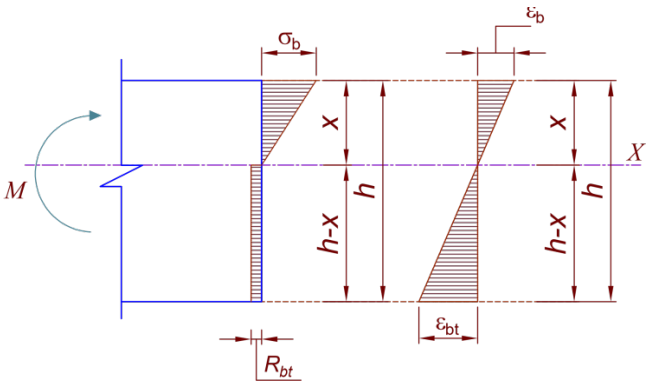

Figure 3. Model of calculation of thick element standard cross-section.
M is bending momentum, h is height of thick element, x is height of compressed zone, R_{bt} is concrete ultimate strength in condition of uniaxial tension, σ_b is normal stress in compression zone.

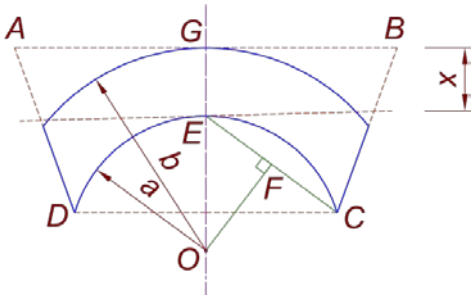

Figure 4. Graphical determination of parameters a&b.

In order to determine numerical values of thick vault inner a and outer b radii it is easy to use to use the model of graphical determination which, due to its demonstrativeness, is practically avoiding occurrence of mistakes (refer to Figure 4).

In [18–20], when analyzing structural strength parameters with account to complex stress state, it was determined that concrete disintegration (in axial compression condition) may occur along the inclined plane. In this case, crack formation begins near the lateral surface supports (Figure 5) with further occurrence of inclined cracks. Further load increase and cracks formation is leading to spherical vault formation.

Experimental investigations of glass and concrete [15, 16] conical elements carried out in late 1970's showed that from the moment of load application and with further load increase the process of crack formation was initiated and continued to spread in upper corner zones of the specimen, near the supports (Figure 2a). With further load increase, performance of the test specimen acquires a different character while stress-strain state transforms to some other qualitative condition. The process of crack formation is shifting from upper corner zones to the lower stretched area of the plate. Evidently, here the supporting sections of the conical element begin to perform in accordance with console-type deformation and it is not useful to take into account their resistance to active loads.

Let us admit that thick plate, prior to crack formation in the lower stretched zone, is performing as a beam, and, as cracks occur and begin spreading, the beam-type behavior is transformed into arc-type (Figure 3) which is characteristic of thick plates.

As it is known [16] – cracked thick axisymmetric plates in spacial deformation state at loads close to ultimate are characterized by formation of considerably large all-round compression area – a peculiar kind of "dome". If we assume the axisymmetric plate in plain deformation state, so the compressed spacial "dome" will transform into a kind of spherical "vault" in which the structure performs as an arc. Therefore, in order to perform analytical calculation of end elements represented by thick plates with consideration of cracked end element's plastic-behavior stage we admit the calculation scheme represented by Figure 5.

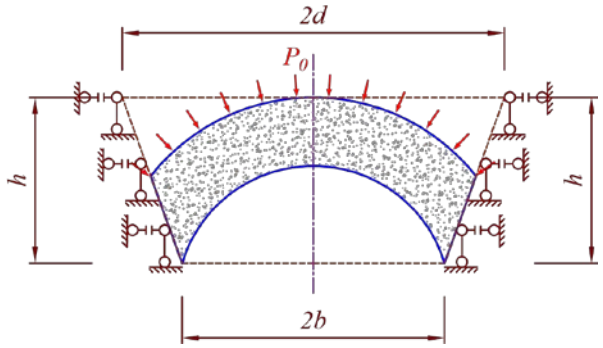

Figure 5. Calculation model for concrete end element.

It is necessary to note that similar model was used for experimental investigation of axisymmetric plate [16], where processes occurring during three-dimensional stress state were expectedly observed.

In the second case, we, tentatively, have relatively small stiffness of the load-bearing wall (Figure 6) where, with increasing operating load, the end elements begin to bias away or to expand the wall in radial direction. At a certain moment, crack formation in lower stretched area of the end elements will begin; at that,

it will begin with formation of standard crack in the middle of element's span (Figure 6a) due to evidently low stiffness of the load bearing wall. At that, thickness of the vault (in comparison with first case) will considerably differ to the smaller size, at that (Figure 6b).

Thus, with low stiffness of the load bearing wall we have low bearing capacity of the end elements.

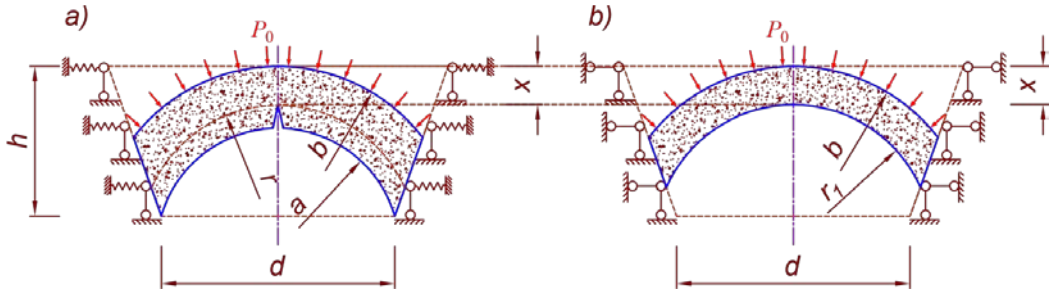

Figure 6. Calculation model for concrete end element with load bearing wall having very low stiffness: a) stage of the normal crack formation and development: *r* is radius of neutral axis b) final stage of formation of spheric vault having small thickness: r_1 is new position of the neutral axis corresponding to static state.

Third case. In order to ensure effective behavior of low-stiffness end elements it is required to use reinforcement (Figure 7*a*). At that, when end elements have sufficient amount of reinforcement metal we can assume that radial displacements may be neglected. Therefore, we can admit (like in the first case) formation of similar stress-strain behavior in the element according to which we will obtain respective calculation model presented in Figure 7b.

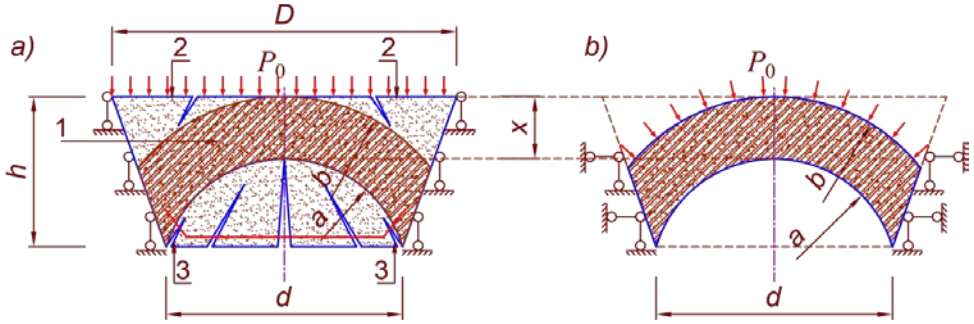

Figure 7. Calculation model. Reinforced concrete end elements with standard load-bearing wall: a) crack formation stage, b) spheric vault formation stage.

It is possible to admit that in this case typical processes (crack occurrence and propagation, formation of vault etc.) will obviously depend on stretched reinforcement behavior under load.

Concrete stiffness [ac. to Balandin] is presented as follows [22]:

$$\sigma_1^2+\sigma_2^2+\sigma_3^2-(\sigma_1\sigma_2+\sigma_2\sigma_3+\sigma_3\sigma_1)-(R_b-R_{bt})(\sigma_1+\sigma_2+\sigma_3)=R_bR_{bt}. \quad (5)$$

Taking into account $\sigma_1=\sigma_2=\sigma_\theta;\ \sigma_3=\sigma_r$ from (5) we obtain

$$(\sigma_1-\sigma_3)^2-(R_b-R_{bt})(2\sigma_1+\sigma_3)=R_bR_{bt}, \quad (6)$$

where σ_1, σ_1, σ_3 are main stresses,

σ_θ, σ_r are accordingly, circumferential and radial stresses,

R_b, R_{bt} are accordingly, concrete ultimate strength in uniaxial compression and tension states.

Differential equation of equilibrium in spherical coordinate system with regard to problem under consideration as per [22]:

$$\frac{d\sigma_r}{dr}+2\frac{\sigma_r-\sigma_\theta}{r}=0. \quad (7)$$

With account to expressions (6) & (7) we obtain

$$\frac{d\sigma_r}{dr}=\frac{1}{r}\cdot\left(2\cdot M+2\cdot\sqrt{M^2+3\cdot M\cdot\sigma_r+N}\right), \quad (8)$$

where $M = R_b - R_{bt}$; $N = R_b R_{bt}$.

We obtain the following boundary conditions for the sphere: at $r = a$, $\sigma_r = 0$ and at $r = b$, $\sigma_r = P_0$.

Further, using "MathCad 15" software quipped with decision function "Odesolve" decision function, with account to admitted boundary conditions and expression (8) we obtain the values of end elements ultimate load and stressed state.

To illustrate usage of dependencies obtained, below given is calculation example.

3. Results and Discussion

Initial data regarding end elements for B40 class concrete [16, 18]: R_b = 22 MPa, R_{bt} = 1.4 MPa, d = 1174 mm, h = 750 mm

We can graphically determine design parameters of the vault: (Figure 4): a = 612 mm; b = 922 mm.

Results of practical calculations are given in Table 1 and demonstrated in Figure 8.

Obtained calculated value of maximum stress: P_0 = 51 MPa.

Figure 8 shows «stress-radius» dependency on the axis of symmetry of the vault.

Table 1. Radial and circumferential stresses depending on radius r.

r, mm	612	643	674	705	736	767	798	829	860	891	922
σ_r, MPa	0	–4	–9	–14	–19	–24	–30	–35	–40	–46	–51
σ_θ, MPa	–42	–52	–62	–71	–80	–89	–98	–107	–115	–124	–132

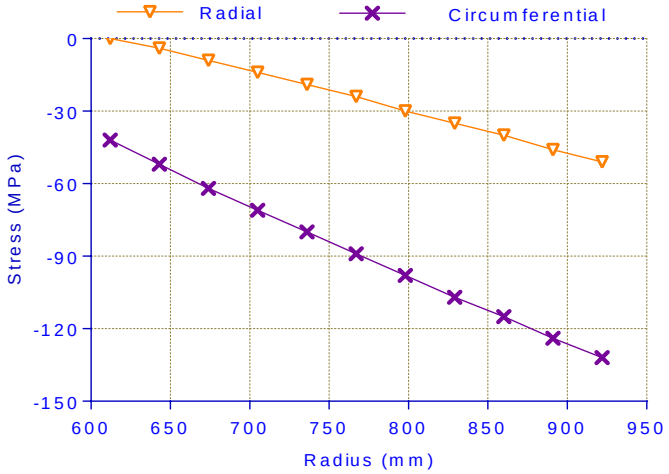

Figure 8. "Stress – radius" dependency diagram.

Development of end elements numerical calculation model with ANSYS WorkBench R18.1 software package [23, 24] will be based on results of analytical calculations made with the use of MathCad 15 software package.

Initial data regarding end elements for B40 class concrete [25]: R_b = 22 MPa, R_{bt} = 1.4 MPa, d = 1174 mm, h = 750 mm, E_b = 36000 MPa, Poison's ratio $\upsilon = 0.18$.

In numerical calculation model we tried to take into account effect of biaxial compression on concrete strength. In this case, under the character of quantitative result evidencing the fact of concrete strength improvement in the state of biaxial compression we assumed the proposal set forth by [19], according to which we obtain the value $R_b^{"} = 35$ MPa for B40 class concrete.

To build a 3D model of a concrete element at which three-axis compression occurs in the program ANSYS Workbench V18.1, we can use one of the following models:

1. Cam-Clay
2. Drucker-Prager
3. Joined Rock

4. Mohr-Coulomb

5. Porous Elasticity

In this article, the Drucker-Prager model for concrete under three-axis compression is chosen for the calculation.

At that, in order to calculate end elements with consideration of load bearing wall made of heavy armored cement, according to [16] let us assume the following initial parameters:

E_r = 44600 MPa, E_θ = 5980 MPa, E_z = 49900 MPa, $\nu_{\theta r}$ = 0.1, $\nu_{\theta z}$ = 0.2, ν_{zr} = 0.28, G = 15600 MPa.

Therefore, for numerical calculation of end elements we used calculation schemes represented by Figure 2, 2a – for vault thickness check, 2b – for stress state check.

Since structure under consideration is axisymmetric and active load is evenly distributed it means that ANSYS numerical method makes use of ¼ 3D-model [26–28]. At that, tangential stresses are represented by "Y"– direction while radial stresses – accordingly by "X" – direction [29–31]. Below given are some results of calculation made with consideration of concrete physical non-linearity.

Figure 9 shows isofields of stresses only in direction "Y" by which it is possible to determine the vault thickness. "+" means stretching, «–» means compression. Stretched zone, in such case, is not covered by calculation

Figure 10 shows tangential stresses in axis of symmetry of the end elements in the following load values: 10 MPa, 20 MPa, 25 MPa, 30 MPa. Please note that height of compressed zone, with increasing external load, is changing rather slightly.

Table 2 gives values of tangential stresses in axis of symmetry of end elements cross sections with reference to various loads and distance. Distance equal to 0 is an outermost fiber of the lower zone, 750 mm – outermost fiber of the upper zone.

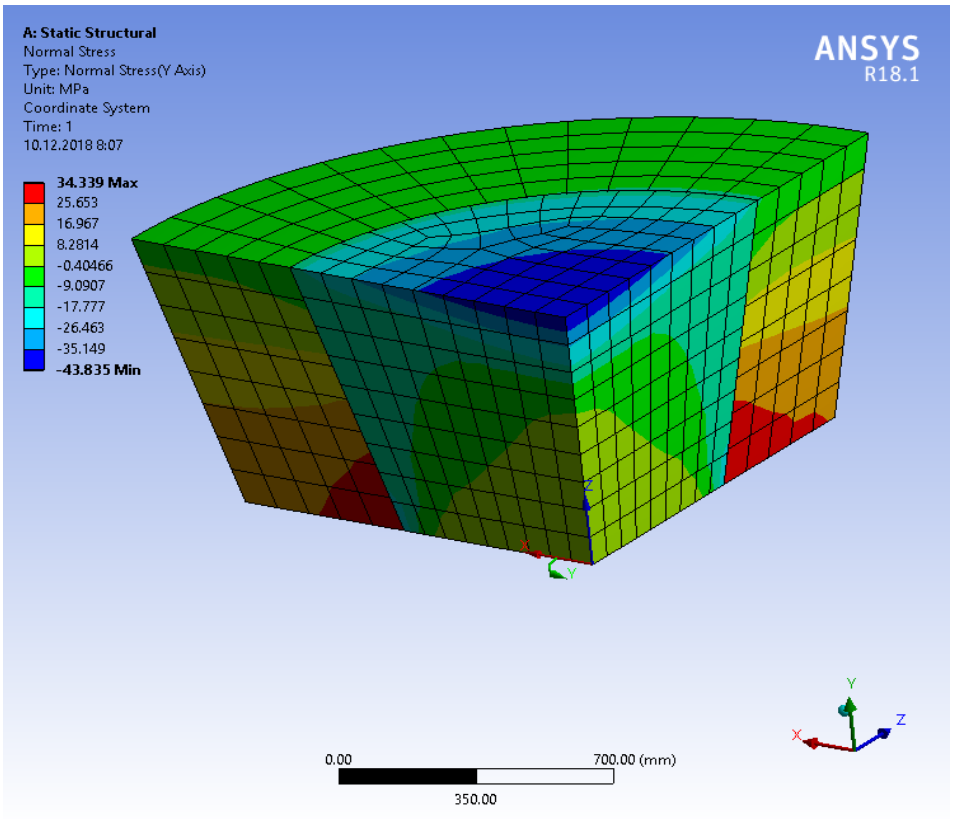

Figure 9. Isofields of stresses in axis "Y"

Table 2. Tangential stresses with reference to load and distance.

Distance,	0	75	150	225	300	375	450	525	600	675	750
10 MPa	1.0	1.0	0.9	0.9	0.9	0.9	0.3	–1.6	–5.1	–8.5	–12.8
20 MPa	1.0	1.0	0.9	0.9	0.9	0.9	0.8	–1.9	–9.9	–18.1	–28.4
25 MPa	1.0	1.0	0.9	0.9	0.9	0.8	0.7	–2.9	–13.0	–23.1	–35.8
30 MPa	0.9	0.9	0.9	0.9	0.9	0.8	–0.2	–5.5	–17.3	–29.1	–43.7

Figures 11, 12 and Tables 3, 4 represent comparison of accordingly radial and tangential stresses for analytical and numerical calculation of the end elements without consideration of the stretched zone.

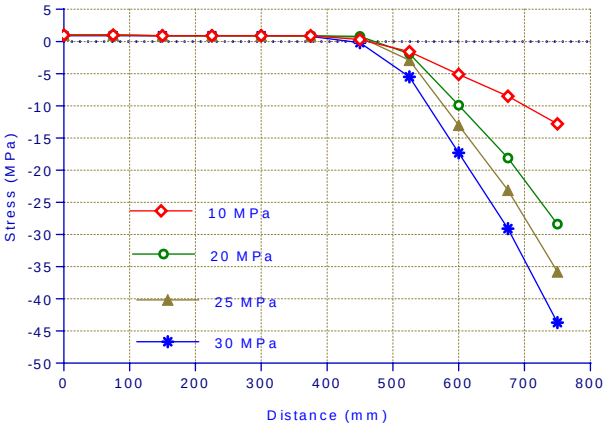

Figure 10. Tangential stresses in symmetry axis of the end elements according to ANSYS.

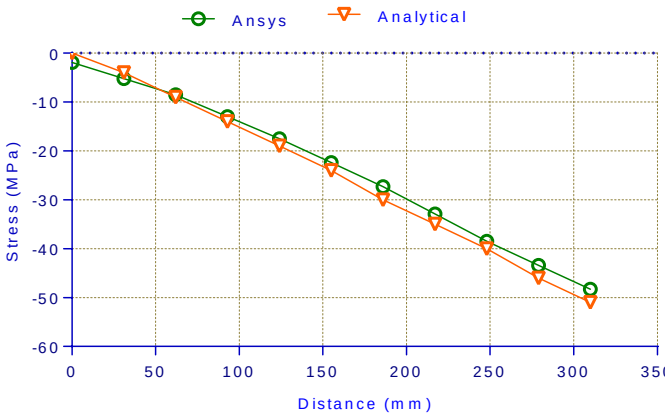

Figure 11. Comparison of radial stresses.

Table 3. Radial stresses in end elements compressed zone.

Distance, mm	0	31	62	93	124	155	186	217	248	279	310
Analytical, MPa	–0	–4	–9	–14	–19	–24	–30	–35	–40	–46	–51
Ansys, MPa	–1.9	–5.2	–8.5	–13.0	–17.5	–22.4	–27.3	–32.9	–38.5	–43.4	–48.3

Table 4. Circumferential stresses in end elements compressed zone.

r, mm	0	31	62	93	124	155	186	217	248	279	310
Analytical, MPa	–42	–52	–62	–71	–80	–89	–98	–107	–115	–124	–132
Ansys, MPa	–35.3	–42.6	–50.0	–60.0	–70.0	–80.9	–91.9	–104.4	–116.8	–127.7	–138.6

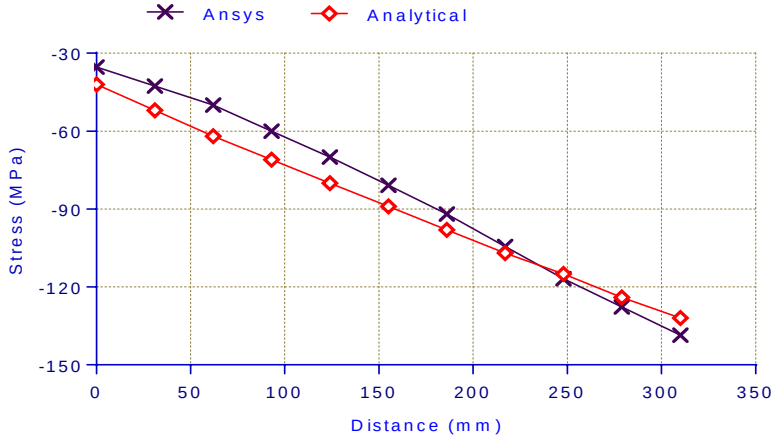

Figure 12. Comparison of circumferential stresses.

Comparison between analytical and numerical calculation models is displaying an essentially reasonable agreement. Moreover, analytical and numerical calculations of the spheric vault formed in the bottom in the course of works give no evident disagreements. Results of comparison between (i) results of analytical calculation of thick sphere and (ii) results of end elements behaviour calculated using ANSYS are unsurprising, i.e. it gives a predicted discrepancy reaching 19 %. This case is stipulated by ANSYS capabilities allowing to consider a more adequate geometrical pattern and, inter alia, to better consider concrete areas which are not made account to in analytical calculation model.

Investigations presented show that concrete end elements affected by cracks occurrence in the stretched area are subjected not to the sudden disintegration but to compressed spheric vault formation. At that, strength of element's spherical vault is more likely depending upon stiffness of load bearing wall – i.e. the lower its stiffness the lower its strength is and vice versa.

Let us note that from Tables 1, 2, 3 and 4 and Figures 11 and 12 we can view that difference between analytical and numerical calculation results is negligeable. Findings obtained cannot deplete the entire scope of issues associated with calculation and designing of this type of structures, however, enable the developer to determine overall dimensions, form and type of reinforcement at the stage of front end engineering design.

4. Conclusions

1. For concrete end elements of the high-pressure casings designed in the form of axisymmetric thick plates affected by ultimate loads and elements naturally affected by triaxial compression are characterized by spheric vault formation.

2. In virtue of assumed allowances and using proximal approach methodology we obtained spheric vault thickness determination formula.

3. Thus, we obtained original models of analytical and numerical calculations allowing to investigate stress state of end elements of high pressure casings designed in the form of axisymmetric thick plates resting on conical surface.

4. Comparison of calculation results obtained with the use of aforesaid methodology shows minor discrepancies (19 %) between analytical and numerical calculation models.

5. Results obtained may be used in design practice – at the stage of high pressure casing front end engineering design.

References

1. Serpik, I.N., Alekseytsev, A.V. Optimization of flat steel frame and foundation posts system. Magazine of Civil Engineering. 2016. 61(1). Pp. 14–24. DOI: 10.5862/MCE.61.2
2. Serpik, I.N., Alekseytsev, A.V., Balabin, P.Yu., Kurchenko, N.S. Flat rod systems: optimization with overall stability control. Magazine of Civil Engineering. 2017. 76(8). Pp. 181–192. DOI: 10.18720/MCE.76.16
3. Rybakov, V.A., Ananeva, I.A., Rodicheva, A.O., Ogidan, O.T. Stress-strain state of composite reinforced concrete slab elements under fire activity. Magazine of Civil Engineering. 2017. 74(6). Pp. 161–174. DOI: 10.18720/MCE.74.13.
4. Alekseytsev, A.V., Kurchenko, N.S. Deformations of steel roof trusses under shock emergency action. Magazine of Civil Engineering. 2017. 73(5). Pp. 3–13. DOI: 10.18720/MCE.73.1
5. Tusnina, O.A., Danilov, A.I. The stiffness of rigid joints of beam with hollow section column. Magazine of Civil Engineering. 2016. 64(4). Pp. 43–55. DOI: 10.5862/MCE.64.4
6. Zinkle, S.J., Busby, T.J. Structural materials for fission & fusion energy. Materials Today. 2009. No. 11(12). Pp. 12–19. DOI: 10.1016/S1369-7021(09)70294-9
7. Klueh, R.L. Reduced-activation bainitic and martensitic steels for nuclear fusion applications. Current Opinion in Solid State Materials Science. 2004. No. 3-4(8). Pp. 239–250. DOI: 10.1016/j.cossms.2004.09.004
8. Klueh, R.L., Hashimoto, N., Maziasz, P. New nano-particle-strengthened ferritic/martensitic steels by conventional thermo-mechanical treatment. Journal of Nuclear Materials. 2007. No. 367–370. Pp. 48–53.
9. Kohyama, A. The development of ferritic steels for DEMO blanket. Fusion Engineering and Design. 1998. No. 41. Pp. 1–6.
10. Blagoeva, D.T., Debarberis, L., Jong, M., Ten Pierick, P. Stability of ferritic steel to higher doses: Survey of reactor pressure vessel steel data and comparison with candidate materials for future nuclear systems. International Journal of Pressure Vessels and Piping. 2014. No. 122. Pp. 1–5. DOI: 10.1016/j.ijpvp.2014.06.001
11. Wang, S. Analytical evaluation of the dome-cylinder interface of nuclear concrete containment subjected to internal pressure and thermal load. Engineering Structures. 2018. 161. Pp. 1–7. DOI: 10.1016/j.engstruct.2018.01.063
12. Bílý, P., Kohoutková, A. Sensitivity analysis of numerical model of prestressed concrete containment. Nuclear Engineering and Design. 2015. No. 295. Pp. 204–214. DOI: 10.1016/j.nucengdes.2015.09.027
13. Hu, H.-T., Lin, J.-X. Ultimate analysis of PWR prestressed concrete containment under long-term prestressing loss. Annals of Nuclear Energy. 2016. No. 87. Part 2. Pp. 500–510. DOI: 10.1016/j.anucene.2015.10.005
14. Becker, G., Steffen, G., Notheisen, C. The design of the prestressed concrete reactor vessel for gas-cooled heating reactors. Nuclear Engineering and Design. 1989. No. 117. Pp. 333–340.
15. Bangash, Y. Safety and reliability of prestressed concrete reactor vessels. Nuclear Engineering and Design. 1979. No. 3(51). Pp. 473–486.
16. Morozov, V.I., Opbul, Eh.K., Van Phuc, P. To the calculation of thick plates of conical plates on the action of uniformly distributed load. Bulletin of Civil Engineers. 2017. No. 2(67). Pp. 66–73. DOI: 10.23968/1999-5571-2018-15-2-66-73
17. Morozov, V.I., Jurij, P. Nuclear Reactor Shell of Heavy Ferrocement. World Applied Sciences Journal. No. 23 (Problems of Architecture and Construction). 2013. Pp. 31–36. DOI: 10.5829/idosi.wasj.2013.23.pac.90007
18. Pukharenko, Yu., Aubakirova, I. Structural features of nanomodified cement stone. Architecture and Engineering. 2016. No. 1(1). Pp. 66–70. DOI: 10.23968/2500-0055-2016-1-1-66-70
19. Rybakov, V.A., Al Ali, M., Panteleev, A.P., Fedotova, K.A., Smirnov, A.V. Bearing capacity of rafter systems made of steel thin-walled structures in attic roofs. Magazine of Civil Engineering. 2017. No. 8. Pp. 28–39. DOI: 10.18720/MCE.76.3.
20. Jiang, J.-F., Xiao, P.-C., Li, B.-B. True-triaxial compressive behaviour of concrete under passive confinement. Construction and Building Materialsr. 2017. No. 156. Pp. 584–598. DOI: 10.1016/j.conbuildmat.2017.08.143
21. Matveeva, L., Efremova, M., Baranets, I. Studies of the morphology of waterproof coatings based on urethane isocyanate, alkyl-phenol-formaldehyde resin and dibutylin dilaurate using the high-resolution optical microscopy technique. Architecture and Engineering. 2018. No. 2(3). Pp. 43–47. DOI: 10.23968/2500-0055-2018-3-2-43-47
22. Andreev, V.I., Potekhin, I.A. Optimization on the strength of thick-walled shells. MGSU. 2011. 86 p.
23. Using ANSYS workbench for structural analysis. Anal. with ANSYS Softw. 2018. Pp. 511–540.

24. Yu, T. Finite element modeling of confined concrete-I: Drucker-Prager type plasticity model. Struct. Elsevier Ltd, 2010. 32(3). Pp. 665–679.
25. Malvar, L.J., Crawford, J.E., Wesevich, J.W. A plasticity concrete material model for DYNA3D. International Journal of Impact Engineering. 1997. No. 19(9-10). Pp. 847–873.
26. Lee, H.-H. Finite Element Simulations with ANSYS Workbench 18 Theory, Applications, Case Studies. 2018. CRC Press, 612 p.
27. Bao, J.Q. et al. A new generalized Drucker-Prager flow rule for concrete under compression. Engineering Structures. 2013. No. 56. Pp. 2076–2082
28. Chen, G., Hao, Y., Hao, H. 3D meso – scale modeling of concrete material in spall tests. Materials and Structures. 2015. No. 48(6). Pp. 1887–1899. DOI: 10.1617/s11527-014-0281-z
29. Babanajad, S.K., Gandomi, A.H., Alavi, A.H. New prediction models for concrete ultimate strength undertrue-triaxial stress states: An evolutionary approach. Advances in Engineering Software. 2017. No. 110. Pp. 55–68. DOI: 10.1016/j.advengsoft.2017.03.011
30. Hokeš, F., Kala, J., Hušek, M., Král, P. Parameter Identification for a Multivariable Nonlinear Constitutive Model inside ANSYS Workbench. Procedia Engineering. 2016. No. 161. Pp. 892–897.
31. Kral, P., Kala, J., Hradil, P. Verification of the elasto-plastic behavior of nonlinear concrete material models. International Journal Mechanics. 2016. No. 10. Pp. 175–181.
32. Chau, V.T., Li, C., Rahimi-Aghdam, S., Bažant, Z.P. The enigma of large-scale permeability of gas shale: Pre-existing or frac-induced? Journal of Applied Mechanics, Transactions ASME. 2017. No. 84(6). DOI: 10.1115/1.4036455
33. Shlyakhin, D.A. Forced axisymmetric vibrations of a thick circular rigidly fixed piezoceramic plate. Mechanics of Solids. 2014. No. 4(49). Pp. 435–444. DOI: 10.3103/S0025654414040086
34. Zhilin, P.A. Axisymmetric bending of a flexible circular plate with large displacements. Mechanics of Solids. 1984. No. 3(19). Pp. 128–134.
35. Wang, Y.Q., Huang, X.B., Li, J. Hydroelastic dynamic analysis of axially moving plates in continuous hot-dip galvanizing process. International Journal of Mechanical Sciences. 2016. No. 110. Pp. 201–216. DOI: 10.1016/j.ijmecsci.2016.03.010
36. Coccia, S., Imperatore, S., Rinaldi, Z. Influence of corrosion on the bond strength of steel rebars in concrete. Materials and Structures. 2016. No. 1-2(49). Pp. 537–551. DOI: 10.1617/s11527-014-0518-x
37. Huang, X., Lu, G., Yu, T. On the axial splitting and curling of circular metal tubes. International Journal of Mechanical Sciences. 2002. No. 11(44). Pp. 2369–2391. DOI: 10.1016/S0020-7403(02)00191-1
38. Zheng, W., Kwan, A.K.H., Lee, P.K.K. Direct tension test of concrete. ACI Materials Journal. 2001. No. 1(98). Pp. 63–71.
39. Stolarski, T., Nakasone, Y., Yoshimoto, S. Engineering Analysis with ANSYS Software (Second Edition). Elsevier. Amsterdam, 2018. 562 p.
40. Alekseytsev, A.V., Akhremenko, S.A. Evolutionary optimization of prestressed steel frames. Magazine of Civil Engineering. 2018. 81(5). Pp. 32–42. DOI: 10.18720/MCE.81.4.
41. Tusnina, O.A., Danilov, A.I. The stiffness of rigid joints of beam with hollow section column. Magazine of Civil Engineering. 2016. 64(4). Pp. 43–55. DOI: 10.5862/MCE.64.4
42. Tusnina, O.A. Finite element analysis of crane secondary truss. Magazine of Civil Engineering. 2018. 77(1). Pp. 68–89. DOI: 10.18720/MCE.77.7

Contacts:

Valery Morozov, +79217907963; morozov@spbgasu.ru
Eres Opbul, +79213170155; fduecnufce@mail.ru
Phan Van Phuc, +79533472586; phucprodhv@gmail.com

Инженерно-строительный журнал

ISSN 2071-0305

сайт журнала: http://engstroy.spbstu.ru/

DOI: 10.18720/MCE.86.9

Работа осесимметричных толстых плит, опертых по конической поверхности

В.И. Морозов*, Э. Опбул, Ф. Ван Фук,
Санкт-Петербургский государственный архитектурно-строительный университет, Санкт-Петербург, Россия

Ключевые слова: корпус высокого давления; торцевой элемент; осесимметричная плита; несущая способность; стенки (структурные элементы); внутреннее давление; нагрузка; шпонка; коническая поверхность.

Аннотация. Настоящая статья посвящена аналитическому и численному исследованиям работы торцовых элементов корпусов высокого давления применительно для ядерных реакторов. Поскольку реальным энергетическим выбором человечества в будущем станет широкое использование ядерной энергии, которая может вырабатываться в корпусах высокого давления, то создание методики расчета торцовых элементов в виде осесимметричных толстых плит, опертых по конической поверхности при действии равномерно распределенной нагрузки, является актуальным. С использованием известных критериев прочности бетона и принятых предпосылок в аналитическом способе расчета, а также на основе численного программного комплекса ANSYS WORKBENCH выполнены расчеты по определению величины предельной нагрузки и напряженного состояния. При этом расчеты выполнены с учетом шпоночного сопряжения толстой плиты с несущей силовой стенкой корпуса высокого давления, в том числе в зависимости от ее достаточно высокой в одном и слабой в другом случаях (переменной) жесткости. Приводится сравнительный анализ результатов расчетов, где обнаруживается адекватность предлагаемых методов расчета. Получены оригинальные способы аналитического и численного расчетов для исследования напряженного состояния торцевых элементов корпусов высокого давления в виде осесимметричных толстых плит, опертых по конической поверхности. Для работы торцевых элементов под нагрузкой свойственно образование сферического свода, где закономерно возникает напряженное состояние, характерное при трехосном сжатии бетона. Приведенные исследования показывают, что в торцевых элементах из бетона с образованием трещин в растянутой зоне не наступает внезапное разрушение, а формируется сжатый сферический свод. При этом прочность сферического свода элемента в большей степени зависит от жесткости несущей силовой стенки: чем меньше жесткость, тем меньше прочность и наоборот. Получены следующие научные результаты: – для торцовых элементов в виде толстых осесимметричных плит в предельных значениях нагрузки характерно образование сферического свода; – на основе принятых допущений, приближенным способом, получена формула по определению толщины сферического свода; – получены оригинальные способы аналитического и численного расчетов для исследования напряженного состояния торцовых элементов корпусов высокого давления в виде осесимметричных толстых плит, опертых по конической поверхности; – сравнение результатов расчетов обнаруживают незначительные расхождения аналитического и численного методов.

Литература

1. Серпик И.Н., Алексейцев А.В. Оптимизация системы стальной плоской рамы и столбчатых фундаментов // Инженерно-строительный журнал. 2016. №1(61). С. 14–24. DOI: 10.5862/MCE.61.2
2. Серпик И.Н., Алексейцев А.В., Балабин П.Ю., Курченко Н.С. Плоские стержневые системы: оптимизация с контролем общей устойчивости // Инженерно-строительный журнал. 2017. № 8(76). С. 181–192. DOI: 10.18720/MCE.76.16
3. Рыбаков В.А., Ананьева И.А., Родичева А.О., Огидан О.Т. Напряженно-деформированное состояние фрагмента сталежелезобетонного перекрытия в условиях огневого воздействия // Инженерно-строительный журнал. 2017. № 6(74). С. 161–174. DOI: 10.18720/MCE.74.13.
4. Алексейцев А.В., Курченко Н.С. Деформации стальных стропильных ферм при ударных аварийных воздействиях // Инженерно-строительный журнал. 2017. № 5(73). С. 3–13. DOI: 10.18720/MCE.73.1

5. Туснина О.А., Данилов А.И. Жесткость рамных узлов сопряжения ригеля с колонной коробчатого сечения // Инженерно-строительный журнал. 2016. № 4(64). С. 40–51. DOI: 10.5862/MCE.64.4
6. Zinkle S.J, Busby T.J. Structural materials for fission & fusion energy // Materials Today. 2009. № 11(12). Pp. 12–19. DOI: 10.1016/S1369-7021(09)70294-9
7. Klueh R.L. Reduced-activation bainitic and martensitic steels for nuclear fusion applications // Current Opinion in Solid State Materials Science. 2004. № 3-4(8). Pp. 239–250. DOI: 10.1016/j.cossms.2004.09.004
8. Klueh R.L., Hashimoto N., Maziasz P. New nano-particle-strengthened ferritic/martensitic steels by conventional thermo-mechanical treatment // Journal of Nuclear Materials. 2007. № 367–370. Pp. 48–53.
9. Kohyama A. The development of ferritic steels for DEMO blanket // Fusion Engineering and Design. 1998. № 41. Pp. 1–6.
10. Blagoeva D.T., Debarberis L., Jong M., Ten Pierick P. Stability of ferritic steel to higher doses: Survey of reactor pressure vessel steel data and comparison with candidate materials for future nuclear systems // International Journal of Pressure Vessels and Piping. 2014. № 122. Pp. 1–5. DOI: 10.1016/j.ijpvp.2014.06.001
11. Wang S. Analytical evaluation of the dome-cylinder interface of nuclear concrete containment subjected to internal pressure and thermal load // Engineering Structures. 2018. № 161. Pp. 1–7. DOI: 10.1016/j.engstruct.2018.01.063
12. Bílý P., Kohoutková A. Sensitivity analysis of numerical model of prestressed concrete containment // Nuclear Engineering and Design. 2015. № 295. Pp. 204–214. DOI: 10.1016/j.nucengdes.2015.09.027
13. Hsuan-Teh H., Jun-Xu L. Ultimate analysis of PWR prestressed concrete containment under long-term prestressing loss // Annals of Nuclear Energy. 2016. № 87. Part 2. Pp. 500–510. DOI: 10.1016/j.anucene.2015.10.005
14. Becker G., Steffen G., Notheisen C. The design of the prestressed concrete reactor vessel for gas-cooled heating reactors // Nuclear Engineering and Design. 1989. № 117. Pp. 333–340.
15. Bangash Y. Safety and reliability of prestressed concrete reactor vessels // Nuclear Engineering and Design. 1979. № 3 (51). Pp. 473–486.
16. Morozov V.I., Pbpublic., Fuk F.V. to the calculation of thick plates of conical plates on the action of uniformly distributed load // Bulletin of civil engineers. 2017. № 2 (67). Pp. 66–73. DOI: 10.23968/1999-5571-2018-15-2-66-73
17. Morozov V.I., Jurij P. Nuclear Reactor Shell of Heavy Ferrocement // World Applied Sciences Journal. № 23 (Problems of Architecture and Construction). 2013. Pp. 31–36. DOI: 10.5829/idosi.wasj.2013.23.pac.90007
18. Pukharenko Yu., Aubakirova I. Structural features of nanomodified cement stone // Architecture and Engineering. 2016. № 1(1). Pp. 66–70. DOI: 10.23968/2500-0055-2016-1-1-66-70
19. Рыбаков В.А., Ал Али М., Пантелеев А.П., Федотова К.А., Смирнов А.В. Несущая способность стропильных систем из стальных тонкостенных конструкций в чердачных крышах // Инженерно-строительный журнал. 2018. № 8(76). С. 28–39. DOI: 10.18720/MCE.76.3.
20. Jiang J., Xiao P., Ben-ben L. True-triaxial compressive behaviour of concrete under passive confinement // Construction and Building Materialsr. 2017. № 156. Pp. 584–598. DOI: 10.1016/j.conbuildmat.2017.08.143
21. Matveeva L., Efremova M., Baranets I. Studies of the morphology of waterproof coatings based on urethane isocyanate, alkyl-phenol-formaldehyde resin and dibutylin dilaurate using the high-resolution optical microscopy technique // Architecture and Engineering. 2018. № 2(3). Pp. 43–47. DOI: 10.23968/2500-0055-2018-3-2-43-47
22. Andreev V.I., Potekhin I.A. optimization on the strength of thick-walled shells. MGSU. 2011. 86 p.
23. Using ANSYS workbench for structural analysis. Anal. with ANSYS Softw. 2018. Pp. 511–540.
24. Yu T. Finite element modeling of confined concrete-I: Drucker-Prager type plasticity model // Struct. Elsevier Ltd, 2010. № 32 (3). Pp. 665–679.
25. Malvar L.J., Crawford J.E.. Wesevich J.W. A plasticity concrete material model for DYNA3D // International Journal of Impact Engineering. 1997. № 19(9-10). Pp. 847–873.
26. Lee H.-H. Finite Element Simulations with ANSYS Workbench 18 Theory // Applications, Case Studies. 2018. CRC Press. 612 p.
27. Bao J. Q. et al. A new generalized Drucker-Prager flow rule for concrete under compression // Engineering Structures. 2013. № 56. Pp. 2076–2082.
28. Chen G., Hao Y., Hao H. 3D meso – scale modeling of concrete material in spall tests // Materials and Structures. 2015. № 48(6). Pp. 1887–1899. DOI: 10.1617/s11527-014-0281-z
29. Babanajad S.K., Gandomi A.H., Alavi A.H. New prediction models for concrete ultimate strength undertrue-triaxial stress states: An evolutionary approach // Advances in Engineering Software. 2017. № 110. Pp. 55–68. DOI: 10.1016/j.advengsoft.2017.03.011
30. Hokeš F., Kala J., Hušek M., Král P. Parameter Identification for a Multivariable Nonlinear Constitutive Model inside ANSYS Workbench // Procedia Engineering. 2016. № 161. Pp. 892–897.
31. Kral P., Kala J., Hradil P. Verification of the elasto-plastic behavior of nonlinear concrete material models // International Journal Mechanics. 2016. № 10. Pp. 175–181.
32. Chau V.T., Li C., Rahimi-Aghdam S., Bažant Z.P. The enigma of large-scale permeability of gas shale: Pre-existing or frac-induced? // Journal of Applied Mechanics, Transactions ASME. 2017. № 84(6). DOI: 10.1115/1.4036455
33. Shlyakhin D.A. Forced axisymmetric vibrations of a thick circular rigidly fixed piezoceramic plate // Mechanics of Solids. 2014. № 4(49). Pp. 435–444. DOI: 10.3103/S0025654414040086
34. Zhilin P.A. Axisymmetric bending of a flexible circular plate with large displacements // Mechanics of Solids. 1984. № 3(19). Pp. 128–134.
35. Wang Y.Q., Huang X.B., Li J. Hydroelastic dynamic analysis of axially moving plates in continuous hot-dip galvanizing process // International Journal of Mechanical Sciences. 2016. № 110. Pp. 201–216. DOI: 10.1016/j.ijmecsci.2016.03.010
36. Coccia S., Imperatore S., Rinaldi, Z. Influence of corrosion on the bond strength of steel rebars in concrete // Materials and Structures. 2016. № 1-2(49). Pp. 537–551. DOI: 10.1617/s11527-014-0518-x

37. Huang X., Lu G., Yu T. On the axial splitting and curling of circular metal tubes // International Journal of Mechanical Sciences. 2002. № 11(44). Pp. 2369–2391. DOI: 10.1016/S0020-7403(02)00191-1

38. Zheng W., Kwan A.K.H., Lee P.K.K. Direct tension test of concrete // ACI Materials Journal. 2001. № 1(98). Pp. 63–71.

39. Stolarski T., Nakasone Y., Yoshimoto S. Engineering Analysis with ANSYS Software (Second Edition). Elsevier. Amsterdam, 2018. 562 p.

40. Алексейцев А.В., Ахременко С.А. Эволюционная оптимизация предварительно напряженных стальных рам // Инженерно-строительный журнал. 2018. № 5(81). С. 32–42. DOI: 10.18720/MCE.81.4.

41. Туснина О.А., Данилов А.И. Жесткость рамных узлов сопряжения ригеля с колонной коробчатого сечения // Инженерно-строительный журнал. 2016. № 4(64). С. 40–51. DOI: 10.5862/MCE.64.4

42. Туснина О.А. Конечно-элементное моделирование и расчёт подкраново-подстропильной фермы // Инженерно-строительный журнал. 2018. № 1(77). С. 68–89. DOI: 10.18720/MCE.77.7

Контактные данные:

Валерий Иванович Морозов, +79217907963; эл. почта: morozov@spbgasu.ru
Эрес Опбул, +79213170155; эл. почта: fduecnufce@mail.ru
Фан Ван Фук, +79533472586; эл. почта: phucprodhv@gmail.com